THE JOURNAL OF PHYSICAL CHEMISTRY B

Article

pubs.acs.org/JPCB

Formation of Surface Relief Gratings: Effect of the Density of the Host Material

V. Teboul*,†,‡ and J. B. Accary†

†LUNAM Université, Université d'Angers, Département de Physique, CNRS UMR 6200, Laboratoire MOLTECH Anjou, 2 Bd Lavoisier, F-49045 Angers, France

‡Department of Chemistry, University of California, Berkeley, California 94720, United States

ABSTRACT: We use molecular dynamics simulations to investigate the effect of the density of the host material on the isomerization-induced diffusion mechanism that results in surface relief gratings formation. We find that a decrease in density increases the diffusion coefficient in a similar way for driven and spontaneous diffusion. This result suggests that the driving mechanism depends only slightly on the density of the host material. The pressure variations during the isomerization process decrease when the driven diffusion increases due to material softening for smaller densities. These results suggest that the pressure variations are not at the origin of the driven motions. The relative local density variation around the probe is also weakly dependent on the mean density of the host material as long as the material structure is preserved.

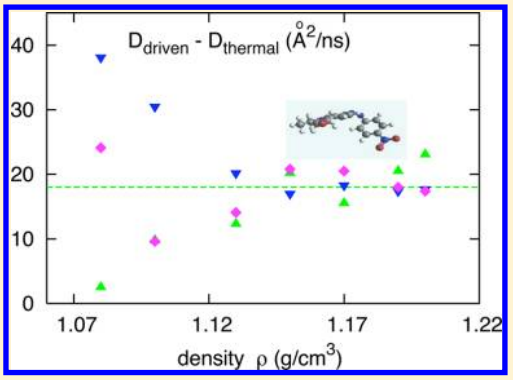

I. INTRODUCTION

Illuminating thin polymer films doped with azo dyes J. P. Rochon, E. Batalla, and A. L. Natansohn[1] and independently D. Y. Kim, S. K. Tripathy, L. Li, and J. Kumar[2] found a massive photoinduced mass transport[3−7] well below the glass transition temperature of the material. Various explanations have been suggested for the underlying microscopic mechanism.[3] One of the most interesting and simple explanations is that the massive motions are induced by pressure gradients inside the material.[3] Indeed, important pressure gradients[8] are produced during isomerization due to the changing shape of the isomerizing probe. Pressure gradients or stress are known to accelerate the dynamics of soft materials[9] in agreement with the model. However, the structure of the material is not modified by the successive isomerizations[1] in opposition with stress-induced softening. The increase of cooperative motions, called dynamical heterogeneity,[10,11] has been reported[12−14] inside the material during isomerization, while stress is known to decrease[9] these cooperative motions. These two contradictions are not sufficient to reject the pressure gradients simple and beautiful explanation. However, it suggests conducting more research in this direction. In this article we use molecular dynamics simulations to investigate the density dependence of the isomerization-driven motions. The main idea behind the study is that a decrease in the density of the host material must decrease the isomerization-induced pressure gradients. Thus, if this model is correct the driven diffusion must decrease and eventually disappear at low enough density.

II. CALCULATION

We present molecular dynamics simulations of the effect of photoisomerization of probe molecules on the dynamics of a glassy molecular material. We simulate the photoisomerization of dispersed red (DR1) probe molecules ($C_{16}H_{18}N_4O_3$, *N*-ethyl-*N*-(2-hydroxyethyl)-4-(4-nitrophenylazo)aniline; CAS number 2872-52-8) inside a matrix of methyl methacrylate (MMA) molecules ($C_5O_2H_8$). The simulation procedure has been described in detail in previous papers.[12,15,16] The MMA potential is however different in this work. In order to increase the simulation efficiency we use a recent coarse grain model[17] for the MMA molecule, while the probe is modeled with a detailed all-atom potential.[18] The density is set constant at 1.19 g/cm^3. The simulation box countains 336 MMA and 7 DR1 molecules. The cubic simulation box is 36.8 Å wide. We use the Gear algorithm with the quaternion method[19] to solve the equations of motions. The potential functions are Lennard−Jones interatomic potentials. Due to the simplicity of these potentials we expect that the results could be qualitatively generalized to a number of other molecules. The time step is 0.5×10^{-15} s. We have chosen this short time scale due to the rapid isomerization process. The temperature is controlled using a Berendsen thermostat.[20] In order to study the effect of the photoisomerization, the DR1 molecules change periodically and continuously from the trans to the cis isomer and then from the cis to the trans isomer. The DR1 molecule changes from trans to cis uniformly in a time t_1 = 300 fs. This value is typical of the isomerization process.[21] Then it stays in the cis configuration during time t_2, changes from cis to trans in time t_1, and stays in the trans configuration during time t_2. Results presented in this article correspond to $t_2 = 20t_1$. During

Received: May 31, 2012
Revised: September 20, 2012

   dx.doi.org/10.1021/jp3053423 | J. Phys. Chem. B XXXX, XXX, XXX−XXX

isomerization, the shape of the DR1 molecule is modified slightly at each time step using the quaternion method with constant quaternion variations, calculated to be in the final trans or cis configuration after a 300 fs isomerization corresponding to 600 time steps. This method corresponds to opposite continuous rotations of the two parts of the molecule that are separated by the nitrogen bounding. We used two rotations with different axes for each part of the molecule in order to obtain isomerization. Due to the change in the conformation of the molecule, the inertia moments and centers of masses of the DR1 molecules are reevaluated at each time step during isomerization. Two different photoisomerization mechanisms[22−24] (rotation around the NN bond or inversion around an N atom) have been reported for the azobenzene molecule. In this work we use the inversion mechanism. However, our results have been found to be qualitatively robust to important changes in the isomerization conditions. The simulations are aged for 1 ns before any treatment. The configurations are then stored and used for statistical calculations. We do not use any smoothing procedure on our curves. The curves thus show the magnitude of the statistical fluctuations which are small due to the large number of configurations (>10 000) averaged. Typical experimental light exposure leads to a value of 1 ms between isomerization events.The waiting time value t_2 used in our simulations (6 ps) is thus very short when compared to the usual experimental times. These differences have been discussed in previous papers.[15,16]

III. RESULTS AND DISCUSSION

For both diffusion mechanisms, Figure 1 shows the mean square displacements (MSD) of the host material for various densities ranging from ρ = 1.08 to 1.2 g/cm^3 at a temperature (T = 140 K) where the liquid is supercooled but still not a glass. For this methylmethacrylate (host material) coarse grain model at a density of ρ = 1.19 g/cm^3 we evaluate the onset temperature to be around T_0 = 300 K with the apparition of a small plateau in the mean square displacement. For T = 140 K the plateau appears around the smallest density considered in the figure, ρ = 1.08 g/cm^3 . Figure 1 shows that the mean square displacements are larger and less dispersed when isomerization is set on. The MSD however follow the same continuous density evolution. When the density increases the MSD decreases whether isomerization is set on (driven diffusion) or off (thermal diffusion). Oscillations appear in the driven MSD for the largest densities displayed. These oscillations follow the isomerization period. For smaller densities these oscillations are masked by the thermal diffusion of the molecules located at a long distance from the probe. Figure 1 shows that the main effect of the density is to decrease the motion of the host material molecules. We do not see any increase of driven motions when the density increases, as may be expected for a pressure gradient driven mechanism. In order to make a more precise comparison we show in Figure 2 the driven and nondriven MSD for two different densities at temperatures corresponding approximately to the same nondriven diffusion coefficient. We chose T = 140 K with ρ = 1.1 g/cm^3 and T = 190 K with ρ = 1.19 g/cm^3. Figure 2 shows that for thermal diffusion the MSD is slightly larger for ρ = 1.19 g/cm^3 and T = 190 K than for ρ = 1.1 g/cm^3 and T = 140 K . On the contrary, the MSD is slightly smaller for ρ = 1.19 g/cm^3 for driven diffusion. This result is in contradiction with a pressure gradient driving mechanism. Figure 3 shows the diffusion coefficient evolution with density at a constant temperature for the driven and thermal diffusions. For both diffusion mechanisms the diffusion coefficient decreases when the density increases. However, the thermal diffusion coefficient $D_{\text{thermal}}(\rho,T)$ decreases more rapidly than its driven counterpart $D_{\text{driven}}(\rho,T)$ at high density. The driven diffusion coefficient $D_{\text{driven}}(\rho,T)$ tends to a limit constant value at high density, while $D_{\text{thermal}}(\rho,T)$ decreases continuously. This result is similar with the temperature evolution of the diffusion coefficient.[12] When the temperature decreases $D_{\text{driven}}(\rho,T)$ tends to a limit constant value while $D_{\text{thermal}}(\rho,T)$ decreases. We also see that for small densities the driven and thermal diffusion merge. This result is also similar to what is seen for large temperatures.[12] These results show that for small densities or large temperatures the thermal diffusion becomes larger than the part of the driven diffusion originating from the driving mechanism. In other words we may write $D_{\text{driven}}(\rho,T)$ as a sum of the thermal diffusion that still exists during isomerization and of a pure

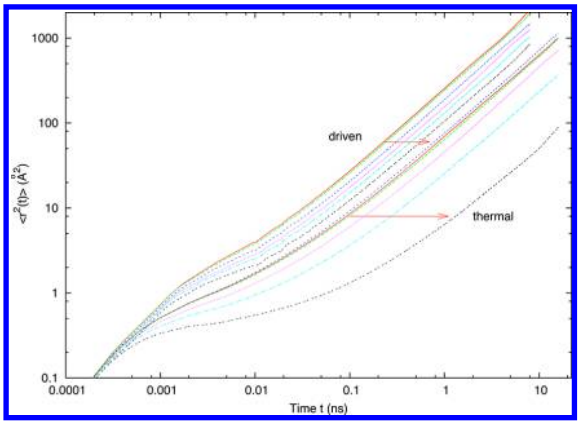

Figure 1. Mean square displacements for various densities at temperature T = 140 K. Upper curves correspond to isomerization set on (driven diffusion). From bottom to top: ρ = 1.2, 1.17, 1.15, 1.13, 1.10, and 1.08 g/cm^3 with isomerization set off (thermal diffusion) and then the same densities for the driven diffusion. Arrows show increasing densities for driven and thermal diffusion.

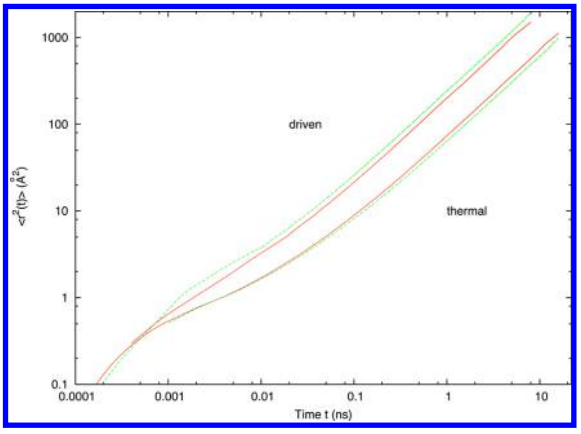

Figure 2. Comparison between the mean square displacements at two different densities for driven and thermal diffusion. Temperatures are adjusted to obtain roughly similar thermal diffusion: (—) T = 140 K and ρ = 1.1 g/cm^3; (- - -) T = 190 K and ρ = 1.19 g/cm^3. Upper curves: driven diffusion. We see that similar thermal diffusion leads to similar driven diffusion. This result suggests that the density does not affect the driving diffusion mechanism.

dx.doi.org/10.1021/jp3053423 | J. Phys. Chem. B XXXX, XXX, XXX−XXX

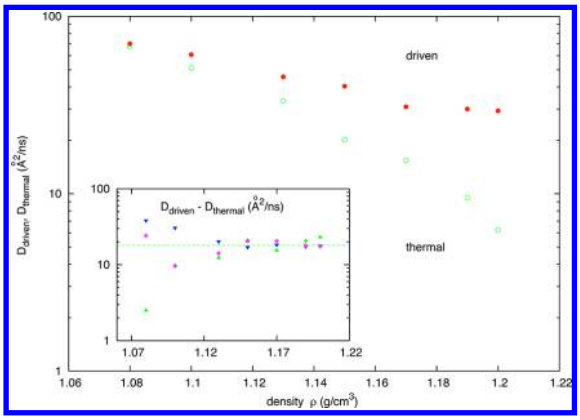

Figure 3. Driven and thermal diffusion coefficients versus density at T = 180 K: (●) driven diffusion; (○) thermal diffusion. When the density increases D_{driven} tends to a limit value while $D_{thermal}$ tends to zero. (Inset) Increase in diffusion due to the driving mechanism $D_{induced} = D_{driven} - D_{thermal}$ versus density at T = 140 (▼), 160 (♦), and 180 K (▲). Uncertainty is larger for the smaller densities because we calculate a small difference between large values. Dashed line corresponds to $D_{induced}$ = 18 Å²/ns. Whole set of points is compatible with the constant driving mechanism displayed by the line when the uncertainties are taken into account.

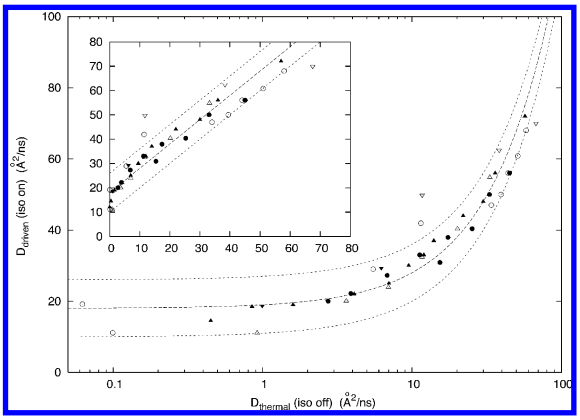

Figure 4. Diffusion coefficient of the host material when isomerization is set on D_{driven} versus the same diffusion coefficient when isomerization is set off $D_{thermal}$ for various temperatures and densities. Density is ρ = 1.08 (▽), 1.1 (○), 1.15 (△), 1.17 (●), 1.19 (▲), and 1.2 g/cm³ (▼). Mean dashed line corresponds to the equation $D_{driven} = D_{thermal} + D_0$ with D_0 = 18 Å²/ns. This line corresponds to a constant effect of the isomerization of 2.5 Å²/ns/probe whatever the density or temperature. This result shows that the density has no effect on the isomerization-induced increase of the diffusion coefficient in the density range studied. Upper (lower) dashed line corresponds to the same equation with D_0 = 26 Å²/ns (10 Å²/ns). (Inset) Same results in a linear scale.

driven contribution $D_{induced}(\rho,T)$: $D_{driven}(\rho,T) = D_{induced}(\rho,T) + D_{thermal}(\rho,T)$. Because $D_{driven}(\rho,T)$ tends to $D_{thermal}(\rho,T)$, we conclude that $D_{induced}(\rho,T) \ll D_{thermal}(\rho,T)$ for low densities or high temperatures. While for high densities or low temperatures $D_{driven}(\rho,T) \gg D_{thermal}(\rho,T)$ shows that $D_{induced}(\rho,T) \gg D_{thermal}(\rho,T)$, i.e., thermal diffusion becomes small and the driving mechanism becomes preponderant. A more precise analysis is shown in the inset. The difference $D_{induced}(\rho,T) = D_{driven}(\rho,T) - D_{thermal}(\rho,T)$ that represents the driving mechanism contribution to the diffusion is plotted versus density for three different temperatures. The first points (the smaller densities) have large uncertainties because they are obtained from the difference of large numbers. For larger densities the difference $D_{induced} = D_{driven}(\rho,T) - D_{thermal}(\rho,T)$ is approximately constant. These results are compatible with a constant driving mechanism (2.5 Å²/ns/probe for the conditions of our simulations) that does not depend on the density or temperature.

When isomerization is set off, a decrease in density or an increase in temperature results in an increase of the diffusion coefficient $D_{thermal}(\rho,T)$. To be able to compare the dynamics for different densities and temperatures we thus have to find a variable that defines the same corresponding states. We will use the thermal diffusion coefficient $D_{thermal}(\rho,T)$ for this purpose. In doing so we make the hypothesis that similar thermal diffusion coefficients means that the dynamics is similar. Figure 4 shows the diffusion coefficient of the host material when the isomerization of the probe is set on (D_{driven}) versus the diffusion coefficient without isomerization ($D_{thermal}$). The different symbols correspond to different densities. The full circles correspond to the highest density in our study and the empty triangles to the lowest. Figure 4 shows that the isomerization-induced diffusion coefficients $D_{driven}(\rho,T)$ are the same for various densities once $D_{thermal}(\rho,T)$ is chosen. The inset shows the same data in a linear scale. The linear dependence of the driven diffusion coefficients $D_{driven}(\rho,T)$ with $D_{thermal}(\rho,T)$ is clear on this plot. Both plots show that the points follow a dashed line that corresponds to the equation $D_{driven} = D_{thermal} + D_0$ with D_0 = 18 Å²/ns. The line corresponds to a constant effect of the isomerization of 2.5 Å²/ns/probe for the whole set of densities and temperatures displayed. These results show that the density does not affect significantly the driving mechanism in the density range studied. At small enough density however we expect this result to break when the probe will not still be able to push the same number of host material molecules. As the pressure increases with density our findings suggest that pressure as well as density do not have a major role in the diffusion-driving mechanism. However, pressure gradients during isomerization may not follow the same evolution. Thus, we now turn to consider the pressure variations that are at the origin of the pressure gradients.

Figure 5 shows the pressure variations ΔP during isomerization versus the diffusion coefficients $D_{driven}(\rho,T)$ or $D_{thermal}(\rho,T)$. These pressure variations are in qualitative agreement with recent experiments on nanospheres.[8] The figure shows that the pressure variations ΔP are roughly constant for small diffusion $D_{driven}(\rho,T)$ or $D_{thermal}(\rho,T)$ and then decrease slightly as diffusion increases. This decrease of ΔP is expected as the material is softening when $D_{thermal}(\rho,T)$ increases due to an increase in temperature or a decrease in density. This result shows that the pressure variations are not increasing with diffusion as will be expected if ΔP was driving the diffusion. Figure 6 shows the local density variations around the probe during the isomerization process. We obtain this local density by integrating the radial distribution function between the probe and the host material on the first or second shell of neighbors during the isomerization process

$$N(R)/N_0(R) = \int_{R_0}^{R} g^{iso}(r)4\pi r^2\,dr \Big/ \int_{R_0}^{R} g^{iso\text{-}off}(r)4\pi r^2\,dr \quad ([1])$$

where R_0 = 0 and R = 8 Å for the first shell of neighbors and R_0 = 8 Å and R = 12 Å for the second shell. The radial distribution functions $g^{iso}(r)$ during the isomerization process and $g^{iso\text{-}off}(r)$

dx.doi.org/10.1021/jp3053423 | J. Phys. Chem. B XXXX, XXX, XXX–XXX

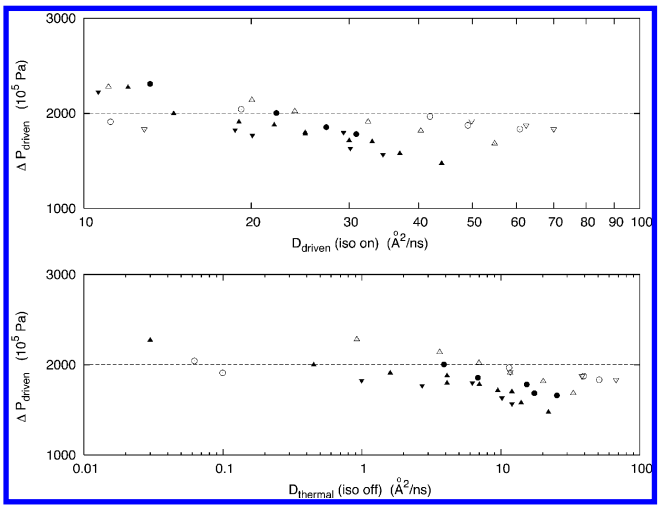

Figure 5. Pressure variations ΔP_{driven} during isomerization versus isomerization-induced D_{driven} or thermal $D_{thermal}$ diffusion coefficients. Pressure is in linear scale, while the diffusion is in logarithmic scale. Same pressure variations lead to very different diffusion coefficients depending on the materials temperature and density. This result suggests that the pressure variations are not the origin of the diffusion mechanism. The density is ρ = 1.08 (▽), 1.1 (○), 1.15 (△), 1.17 (●), 1.19 (▲), and 1.2 g/cm^3 (▼).

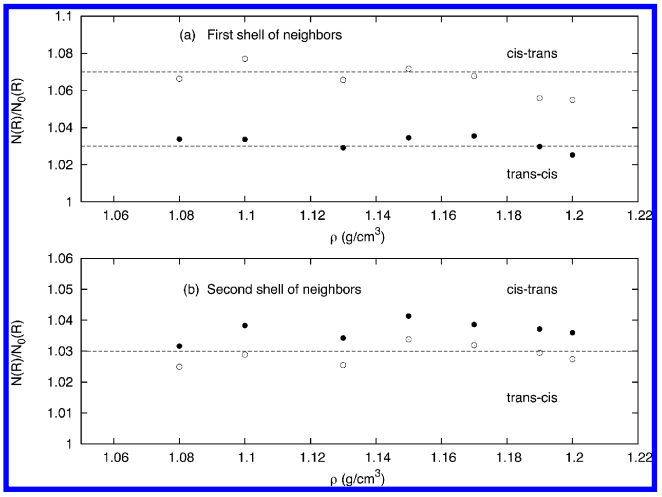

Figure 6. Relative local density $n(R) = N(R)/N_0(R)$ around the probe versus density during isomerization for the two first shells of neighbors: (●) trans−cis isomerization, (○) cis−trans isomerization. (a) First shell of neighbors ($0 < r < 8$ Å). $N(R) = \int_0^{R=8Å} g^{iso}(r) 4\pi r^2 \, dr$ is the local density during isomerization and $N_0(r)$ is the local density when isomerization is set off at the same global density. (b) Second shell of neighbors ($8 < r < 12$ Å). Relative increases of the local densities during isomerization are almost constant in the density range studied. Cis−trans isomerization increases the first-shell relative number of molecules by 7% and the trans−cis isomerization by 3%.

are displayed in Figures 7 and 8 at different densities for the sake of clarity. Figure 6 shows that the density variations for the first shell are 5% for the cis−trans isomerization and 0.6% for the trans−cis isomerization. Both correspond to an increase of the density around the probe during isomerization, in agreement with the observed increase of pressure during isomerization. The first shell density variation is larger for the cis−trans isomerization. However, in our simulations the induced molecular motions are not larger for that isomerization than for the reverse one.[16] Figures 7 and 8 show that during the

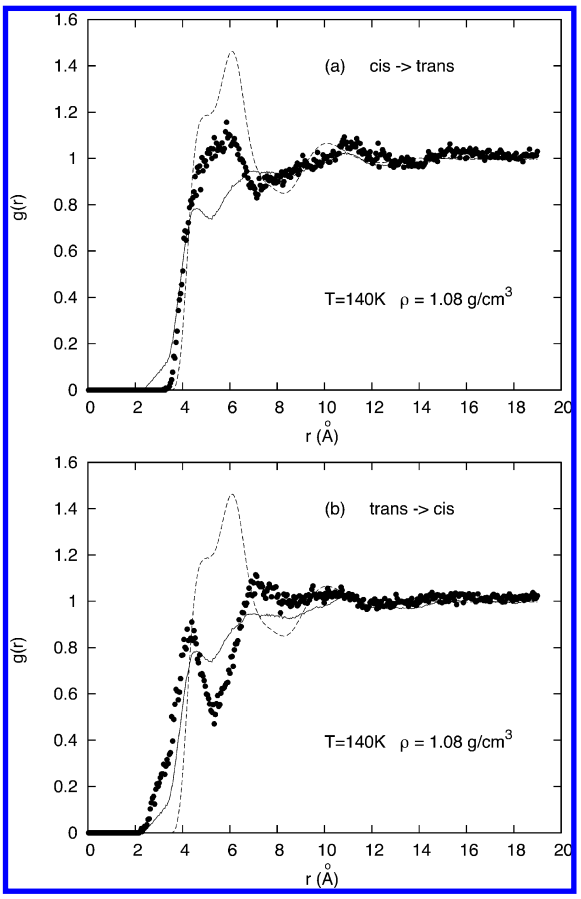

Figure 7. Radial distribution function $g_{probe-matrix}(r)$ between the centers-of-mass of the probe and matrix molecules: (—) $g^{iso-off}_{probe-matrix}(r)$ when isomerization is set off; (●) $g^{iso-on}_{probe-matrix}(r)$ during the cis to trans (a) or trans to cis (b) isomerization process. We also show for comparison (- - -) the radial distribution function $g^{iso-off}_{probe-matrix}(r)$ between the centers-of-mass of the matrix molecules. Density is ρ = 1.08 g/cm^3, and the temperature is T = 140 K.

cis−trans isomerization some matrix molecules approach the probe. As a result we have seen in Figure 6 that the number of molecules in the first shell of neighbors surrounding the probe increases. Then during the trans−cis isomerization a deep decrease develops in the first shell while the second shell increases. Thus, during trans−cis isomerization some molecules are pushed away to the second shell of neighbors, in agreement with a cage-breaking model.[16] Figures 7 and 8 correspond to the lowest and highest densities of this study. These two figures display however quite similar behaviors. This result suggests that the density effect on the isomerization-induced processes is small in the density range studied.

IV. CONCLUSION

Our results show that the density has only slight effects on the isomerization-induced mechanism at the origin of the driven diffusion. This result is amazing as a smaller density implies smaller pressure gradients and forces inside the medium. This result suggests that pressure gradients are not the main origin of the driven diffusion. A smaller density also implies a less structured medium that will result in easier diffusion. Our findings are compatible with a cage-breaking mechanism[16] at the origin of the diffusion. In this view the probe isomerization pushes some molecules from the first to the second probe neighbor shell inducing diffusion. Thus, the diffusion efficiency

dx.doi.org/10.1021/jp3053423 | J. Phys. Chem. B XXXX, XXX, XXX−XXX

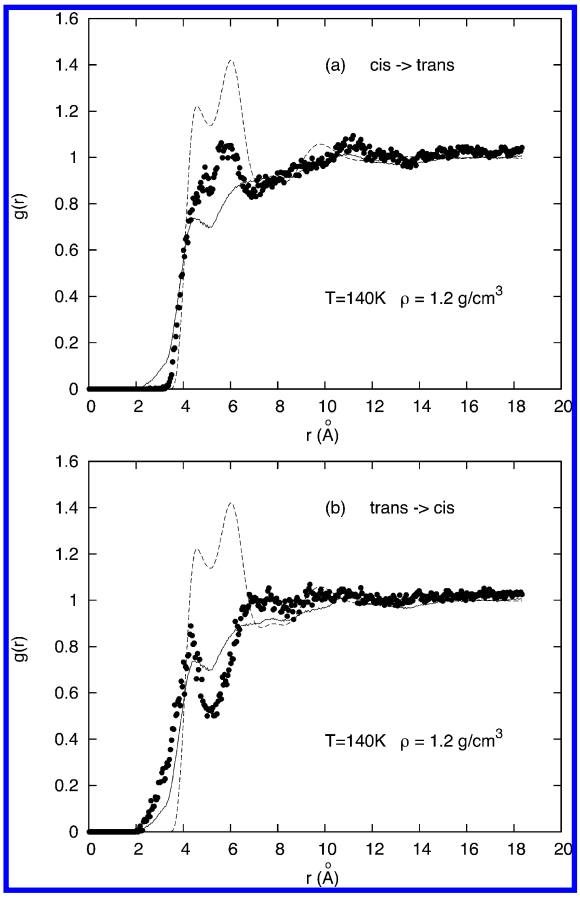

Figure 8. As in Figure 7 but for density ρ = 1.2 g/cm^3.

is not related to the density or pressure but to the number of molecules that can be pushed away by the probe. The relative size of the probe and surrounding molecules will thus be the control parameter. Work is in progress to verify this hypothesis.

AUTHOR INFORMATION

Corresponding Author

*E-mail: victor.teboul@univ-angers.fr.

Notes

The authors declare no competing financial interest.

ACKNOWLEDGMENTS

We want to acknowledge interesting discussions with the Chandler's group in Berkeley, David Chandler, Aaron Keys, David Limmer, Alex Hudson, Kelsey Schuster, Frank Lin, and Prof. Ove Anderson in Umea, and Prof. Jean-Luc Fillaut in Rennes at the beginning of this work. We also aknowledge financial support of the Angers University Ariane grant.

REFERENCES

(1) Rochon, P. L.; Batalla, E.; Natansohn, A. L. *Appl. Phys. Lett.* **1995**, *66*, 136.
(2) Kim, D. Y.; Tripathy, S. K.; Li, L.; Kumar, J. *Appl. Phys. Lett.* **1995**, *66*, 1166.
(3) Natansohn, A.; Rochon, P. *Chem. Rev.* **2002**, *102*, 4139.
(4) Delaire, J. A.; Nakatani, K. *Chem. Rev.* **2000**, *100*, 1817.
(5) Kumar, G. S.; Neckers, D. C. *Chem. Rev.* **1989**, *89*, 1915.
(6) Yager, K. G.; Barrett, C. J. *Curr. Opin. Solid State Mater. Sci.* **2001**, *5*, 487.
(7) Karageorgiev, P.; Neher, D.; Schulz, B.; Stiller, B.; Pietsch, U.; Giersig, M.; Brehmer, L. *Nat. Mater.* **2005**, *4*, 699−703.
(8) Barille, R.; Tajalli, P.; Kucharski, S.; Ortyl, E.; Nunzi, J. M. *Appl. Phys. Lett.* **2010**, *96*, 163104.
(9) Cipelletti, L.; Ramos, L. *J. Phys.: Condens. Matter* **2005**, *17*, R253.
(10) Berthier, L.; Biroli, G.; Bouchaud, J.-P. ; Cipelletti, L.; Van Saarloos, W. *Dynamical heterogeneities in glasses, colloids and granular media*; Oxford University Press: New York, 2011.
(11) Binder, K.; Kob, W. *Glassy materials and disordered solids*; World Scientific: Singapore, 2011.
(12) Teboul, V.; Saiddine, M.; Nunzi, J. M. *Phys. Rev. Lett.* **2009**, *103*, 265701.
(13) Orsi, D.; Cristofolini, L.; Fontana, M. P.; Madsen, A.; Fluerasu, A.; arXiv 1004.1135.
(14) Orsi, D.; Cristofolini, L.; Fontana, M. P.; Pontecorvo, E.; Caronna, C.; Fluerasu, A.; Zontone, F.; Madsen, A. *Phys. Rev. E* **2010**, *82*, 031804.
(15) Saiddine, M.; Teboul, V.; Nunzi, J. M. *J. Chem. Phys.* **2010**, *133*, 044902.
(16) Teboul, V.; Saiddine, M.; Nunzi, J. M.; Accary, J. B. *J. Chem. Phys.* **2011**, *134*, 114517.
(17) Accary, J. B.; Teboul, V. *J. Chem. Phys.* **2012**, *136*, 094502.
(18) Jorgensen, W. L.; Maxwell, D. S.; Tirado-Rives, J. *J. Am. Chem. Soc.* **1996**, *118*, 11225.
(19) Allen, M. P.; Tildesley, D. J. *Computer simulation of liquids*; Oxford University Press: New York, 1990.
(20) Berendsen, H. J. C.; Postma, J. P. M.; Van Gunsteren, W.; DiNola, A.; Haak, J. R. *J. Chem. Phys.* **1984**, *81*, 3684.
(21) Stuart, C. M.; Frontiera, R. M.; Mathies, R. A. *J. Phys. Chem. A* **2007**, *111*, 12072.
(22) Ootani, Y.; Satoh, K.; Nakayama, A.; Noro, T.; Taketsugu, T. *J. Chem. Phys.* **2009**, *131*, 194306.
(23) Fujino, T.; Arzhantsev, S. Y.; Tahara, T. *J. Phys. Chem. A* **2001**, *105*, 8123.
(24) Tiberio, G.; Muccioli, L.; Berardi, R.; Zannoni, C. *Chem. Phys. Chem.* **2010**, *11*, 1018.